16TH EUROPEAN CONFERENCE ON EARTHQUAKE ENGINEERING THESSALONIKI 18 - 21 JUNE 2018

ROLE OF THE EARTHQUAKE SCENARIO ON LIFE-CYCLE SEISMIC RESILIENCE OF AGING BRIDGE NETWORKS

Luca Capacci[1], Fabio Biondini[2]

ABSTRACT

The time-variant structural capacity of critical infrastructure facilities is an important performance indicator in the definition of reliable policies for emergency management and long-term planning of risk mitigation strategies. This paper investigates the seismic resilience of transportation road networks based on a probabilistic framework for life-cycle seismic assessment of deteriorating bridges under prescribed earthquake scenarios with different magnitude and epicenter location. The seismic damage suffered by the exposed bridges and the effects of repair actions are related to traffic limitations and vehicle restrictions implemented over the network. The life-cycle seismic resilience is evaluated under post-event structural recovery of each bridge processes and functionality restoration of the network traffic capacity. The proposed framework is applied to reinforced concrete bridges exposed to seismic hazard and chloride-induced corrosion in a highway network with detour and re-entry link. The results emphasize the role of network topology, earthquake scenario, and time-variant structural deterioration of spatially distributed bridges on the life-cycle functionality and seismic resilience of aging road networks.

Keywords: Bridges; Road networks; Seismic resilience; Earthquake scenario; Environmental hazard; Life-cycle.

1. INTRODUCTION

The definition of proper lifeline management policies is an important task to satisfy the primary needs of communities under full operational conditions, as well as in a state of emergency after extreme events such as earthquakes. Road networks play a key role in the emergency response to seismic events and related hazards, to ensure both quick deployment of aids and resources to distressed communities and prompt repair of the surrounding lifelines and buildings. Bridges are the most vulnerable components of the road networks and suitable levels of seismic capacity and effective repair strategies are necessary to ensure adequate resilience of any community (Carturan *et al.* 2013, Zanini *et al.* 2017).
Resilience is becoming a driving concept for the new generation of structural design codes and standards, informing innovative trends for design, assessment, monitoring and maintenance of strategic facilities and infrastructure systems. Different definitions of resilience can be found in literature, mainly based on the epistemological orientation and theoretical background of the reference discipline (Gilbert 2010). In civil engineering, resilience is usually defined as the capability of a system to withstand the effects of extreme events and to recover promptly and efficiently the pre-event performance and functionality (Bruneau *et al.* 2003). Resilience of structure and infrastructure systems is generally investigated considering sudden damage and disruptions caused by extreme events, such as earthquakes (Cimellaro *et al.* 2010, Decò *et al.* 2013, Titi *et al.* 2015, Franchin and Cavalieri 2015). Natural hazards are often defined in terms of the event magnitude. The seismic risk assessment of vulnerable structures, however, should be informed by several critical factors, including the uncertain distance from the site of the earthquake source (Cornell 1968). In addition, damage and disruptions can also arise continuously in time due to the effects of aging and structural deterioration associated with the exposure of materials, components, and systems to aggressive environment. Consequently, seismic resilience of deteriorating bridges and infrastructure networks depends on the time of occurrence of the seismic event and earthquake scenario (Titi and Biondini 2013, Biondini *et al.* 2015a, 2017, Capacci *et al.* 2016).

[1]PhD Candidate, Dept. of Civil & Environmental Engineering, Politecnico di Milano, Italy, luca.capacci@polimi.it
[2]Professor, Dept. of Civil & Environmental Engineering, Politecnico di Milano, Italy, fabio.biondini@polimi.it

This paper presents a probabilistic approach to life-cycle seismic assessment of bridge structures and resilience analysis of road networks considering the role of the earthquake scenario related to the seismic area source and taking into account the interaction of seismic and environmental hazards. The time-variant seismic fragilities of the deteriorating bridges in the network are assessed through nonlinear incremental dynamic analysis and Monte Carlo simulation with reference to several bridge limit states, from damage limitation up to collapse. The post-event seismic damage and the progressive recovery of seismic performance due to repair actions are related to traffic limitations and vehicle restrictions. The time-variant system functionality is assessed by means of traffic analysis and, finally, life-cycle seismic resilience of the transportation network is quantified. The proposed approach is applied to reinforced concrete (RC) bridges exposed to chloride-induced corrosion in a highway network with detour and re-entry link. Different area sources of seismic hazard are considered to investigate the role of geographical location and spatial distribution of bridges in the road network. The application shows the detrimental effects of aging and structural deterioration of each vulnerable bridge at the network scale and emphasize the importance of the earthquake scenario in a multi-hazard life-cycle-oriented approach to seismic design and assessment of resilient structures and infrastructure systems.

2. LIFETIME SEISMIC ASSESSMENT OF SPATIALLY DISTRIBUTED RC BRIDGES

2.1 Seismic Capacity

2.1.1 Limit States and Fragility Curves

The seismic capacity of RC bridges under uncertainty is evaluated through probabilistic nonlinear incremental dynamic analysis (Vamvatsikos and Cornell 2002). The peak ground acceleration at the b-th bridge location is assumed as seismic intensity measure i_b. The damage measure is the maximum drift $\theta_{\max,b}$, i.e. the maximum ratio of the pier top displacement to the pier height. Limit states are informed by damage limitation, with bridge damage states s_b=0,1,2,3 associated with the drift thresholds listed in Table 1, with $\theta_{p,b}=\theta_{u,b}-\theta_{y,b}$ and where $\theta_{y,b}$ and $\theta_{u,b}$ are the drifts leading to first yielding and ultimate bending curvatures, respectively, at the base of the bridge piers (Capacci 2015). A structural collapse limit state, with s_b=4, is associated with the loss of dynamic equilibrium.

Table 1. Definition of damage states and limit conditions.

Damage State	Acronym	s_b	Limit Condition
No Damage	ND	0	$\theta_{\max,b} < \theta_{y,b}$
Slight Damage	SD	1	$\theta_{\max,b} \geq \theta_{y,b}$
Moderate Damage	MD	2	$\theta_{\max,b} \geq \theta_{y,b}+0.3\theta_{p,b}$
Extensive Damage	ED	3	$\theta_{\max,b} \geq \theta_{y,b}+0.6\theta_{p,b}$
Structural Collapse	SC	4	Loss of dynamic equilibrium

2.1.2 Corrosion Modeling

The main effect of corrosion in RC structures is the reduction of the cross-section of reinforcing steel bars (Bertolini *et al.* 2004). The steel mass loss is measured by a damage index $\delta_s \in [0,1]$ (Biondini *et al.* 2004). Corrosion may also cause a significant reduction of steel ductility. This effect is related to the steel mass loss δ_s by means of a reduction of the ultimate steel strain $\varepsilon_{su}=\varepsilon_{su}(\delta_s)$ (Biondini and Vergani 2015). It is worth noting that the formation of oxidation products may lead to propagation of longitudinal splitting cracks and concrete cover spalling. However, the deterioration of concrete is not considered as a critical issue for the proposed application and it is hence neglected in this paper. Corrosion initiation is associated with a critical threshold of concentration C_{cr} and the corrosion rate is related to chloride concentration $C=C(t)$ by means of a damage rate coefficient q_s. Chloride ingress is described by the Fick's laws of diffusion and evaluated numerically by means of cellular automata (Biondini *et al.* 2004).

2.1.3 Time-variant Bridge Fragilities

The seismic capacity associated with the bridge damage states is investigated under uncertainty in terms of bridge fragility functions $P^E_{s,b}$, i.e. the probability of exceedance of limit states s_b given the occurrence of a seismic event of intensity i_b at time t_0. For RC bridges exposed to chloride-induced corrosion the seismic capacity is time-variant and fragility curves depend on the occurrence time t_0 (Biondini *et al.* 2016, 2017). In this paper, the results of the incremental dynamic analysis are processed for each bridge in the network by assuming lognormal distribution of the fragility functions depending on the bridge age $t_b=t_0-t_{c,b}$, where $t_{c,b}$ is the bridge construction time (Capacci and Biondini 2018a):

$$P^E_{s,b} = P(s_b|i_b,t_b) = \Phi\left(\frac{\ln i_b - \lambda_{s,b}(t_b)}{\zeta_{s,b}(t_b)}\right) \tag{1}$$

where Φ is the standard normal cumulative distribution function, and $\lambda_{s,b}$ and $\zeta_{s,b}$ are the time-variant mean and standard deviation, respectively, of the logarithm of the seismic capacity for damage state s_b.

2.1.4 Marginal and Joint Damage Probabilities

Assuming that $P^E_{0,b}=1$ and $P^E_{5,b}=0$, the time-variant marginal probability of occurrence of the damage $s_b=0,1,2,3,4$ on the b-th bridge given the seismic intensity i_b is defined based on the fragility curves:

$$P_{s,b} = P(s_b|i_b,t_0) = P^E_{s,b} - P^E_{(s+1),b} \tag{2}$$

For a bridge network, each damage state combination can be defined by means of an index s, inspired by the ordered selection without repetitions of the damage states of each bridge s_b, as follows:

$$s = 1 + \sum_b^{N_b} \left(N_{s,b}\right)^{N_b-b} \cdot s_b \tag{3}$$

where N_b is the number of bridges in the network and $N_{s,b}$ is the number of possible damage states for each bridge. Therefore, the total number of network damage state combinations N_s is obtained:

$$N_s = \left(N_{s,b}\right)^{N_b} \tag{4}$$

The time-variant probability of occurrence of the s-th damage combination depends on the seismic event intensity i_b, location $\mathbf{x}_b$ and age t_b of each bridge, as well as on the correlation between the seismic capacities of each pair of bridges. The role of correlation is investigated in Capacci and Biondini (2018b). In this paper, perfect correlation is assumed and the probability associated with the damage combination s is defined based on the multiplication rule of probability theory as follows:

$$P_s = P\left(s_1, s_2, s_3, \dots, s_{N_b}\right) = P\left(s_2, s_3, \dots, s_{N_b}|s_1\right) \cdot P\left(s_3, \dots, s_{N_b}|s_2\right) \cdot \dots \cdot P\left(s_{N_b}\right) \tag{5}$$

Such probabilities will be assumed in the proposed framework as weighing coefficients in the evaluation of the time-variant road network seismic resilience under prescribed earthquake scenarios.

2.2 Ground Motion Prediction and Seismic Area Source

The seismic intensity i_b at the site $\mathbf{x}_b$ of the b-th bridge in the network is related to the seismic scenario in terms of magnitude M and focal distance between bridge site $\mathbf{x}_b$ and epicenter location $\mathbf{x}_e$ based on the ground motion prediction equation proposed by Bindi *et al.* (2011). For the given road networks, characterized by location $\mathbf{x}_b$ and age t_b of each bridge, the joint damage probability depends on the seismic scenario in terms of earthquake magnitude M and epicenter location $\mathbf{x}_e$:

$$P_s = P(s|t_b,i_b) = P(s|\mathbf{x}_b,t_b,M,\mathbf{x}_e) \tag{6}$$

Furthermore, area sources are often used in practice to account for "background" seismicity (Baker 2008) and they can model the seismic exposure of regions characterized by lack of information on the local active faults. Assuming that the likelihood of occurrence of a seismic event with given magnitude is equal in any point of the area source A_s, the uniform probability density function associated with the epicenter location can be conveniently defined as follows:

$$f_{X_e}(\mathbf{x}_e) = \frac{I(\mathbf{x}_e)}{A_s} \tag{7}$$

where $I(\mathbf{x}_e)$ is a step function with $I(\mathbf{x}_e)=1$ if the epicenter location lies within the area source, i.e. $\mathbf{x}_e \in A_s$, and $I(\mathbf{x}_e)=0$ otherwise. Therefore, the joint damage conditional probability associated with bridge locations $\mathbf{x}_b$, bridge ages t_b, and earthquake magnitude M can be evaluated over the seismic area source A_s based on the total probability theorem as follows:

$$P_{s,A} = P_{s,A}(s|\mathbf{x}_b, t_b, M, A_s) = \int_{A_s} P_s(s|\mathbf{x}_b, t_b, M, \mathbf{x}_e) \cdot f_{X_e}(\mathbf{x}_e) \cdot dA \tag{8}$$

3. SEISMIC RESILIENCE OF ROAD NETWORKS

3.1 Network Functionality

3.1.1 Travel Time and Traffic Flow

Consistently with graph theory, a road network is defined as a set of nodes and edges, i.e. vertices and arcs, respectively. Vertices are associated with trip origins and destinations in the transportation system, and edges represent road segments and bridges in series connecting pairs of nodes. The performance and functionality of road networks can be assessed based on traffic flow response and minimum travel time (Bocchini and Frangopol 2011). The travel time c_{ij} of the arc *i-j* can be expressed as:

$$c_{ij} = c_{ij}^0 \left[1 + \alpha \left(f_{ij} \Big/ f_{ij}^{cr}\right)^{\beta}\right] \tag{9}$$

where f_{ij} is the vehicle flow per unit of time in the arc *i-j*, $c^0_{ij} = L_{ij}/v_{lim}$ is the travel time at free flow, $f^{cr}_{ij} = n_L(v_{cr}/d_{\min})$ is the practical capacity, α=0.15, and β=4 (Martin and McGuckin 1998). The parameters c^0_{ij} and f^{cr}_{ij} are traffic capacity coefficients affecting the arc practicability. They depend on the arc length L_{ij}, number of lanes n_L, and arc road class associated with the minimum distance $d_{\min}$ between vehicles, the corresponding speed limit, or critical speed v_{cr}, and the maximum speed limit v_{lim} (Capacci 2015).

3.1.2 Type of Users and Traffic Limitations

The actual practicability of each arc depends on the set of restrictions that the owner of the transportation network imposes to regulate the traffic along each bridge damaged by hazardous events. Restrictions to each type of vehicle and limitations to road traffic capacity are applied depending on the damage state of the bridges in the network (Mackie and Stojadinović 2006). The vehicle flow of three different types of traffic users is considered: light vehicles f_l, heavy vehicles f_h, and emergency vehicles f_e. Traffic limitations in each bridge are identified by a decision variable d_b.
The network restriction combinations d can be expressed in terms of the decision variable d_b of each bridge consistently with the criterion proposed for the damage state combinations:

$$d = 1 + \sum_b^{N_b} \left(N_{d,b}\right)^{N_b - b} \cdot d_b \tag{10}$$

where $N_{d,b}$ is the number of possible states of the decision variable d_b.

The total number of network damage state combinations N_d is hence evaluated as follows:

$$N_d = \left(N_{d,b}\right)^{N_b} \tag{11}$$

The set of possible states of the bridge decision variable d_b considered in this paper are listed in Table 2, where the restrictions $d_b=k$ with $k>1$ are inclusive of the traffic limitations associated with $d_b<k$.

Table 2. Definition of damage states and limit conditions.

Decision Variable	#	Traffic Limitation
No Restrictions	0	$v_{lim}=v_{\max}$
Weight Restriction	1	$f_h=0$ and $v_{lim}=v_{\min}$
One Lane Open Only	2	$n_L=1$
Emergency Access Only	3	$f_e=0$
Closure	4	$f_l=0$ or $n_L=0$

3.1.3 Traffic Analysis and Network Functionality

Given the Origin-Destination (OD) traffic demand, network topology, and arc parameters, the actual traffic flow distribution in each road can be identified based on the user-equilibrium condition enforced by the Wardrop's gravitational model (Wardrop 1952). This model consists in the minimization of the total travel time *TTT* of all the users of the highway network. More details concerning with the solution of the related optimization problem and the definition of the total travel time for a given combination of decision variables $TTT_d=TTT(d)$ can be found in Bocchini and Frangopol (2011) and Capacci (2015).
The functionality level $Q_d=Q(d)\in[0,1]$ of the road network associated with the combination d of network restrictions is defined as follows (Capacci 2015):

$$Q(d) = \frac{TTT_u}{TTT_d} \tag{12}$$

where $TTT_u=TTT(d=1)$ is the total travel time in unrestricted conditions, i.e. no traffic regulations are applied to any bridge. The condition of unrestricted transit with $TTT_d=TTT_u$ and $Q=1$ holds for the network with all bridges under no damage state, that is fulfilled before the occurrence of significant structural deterioration or seismic damage and after recovery processes with bridges fully restored.

3.2 Damage Recovery and Seismic Resilience

3.2.1 Bridge Recovery Process

Bridges may suffer a loss of structural capacity when earthquakes occur. The initial restrictions in the aftermath of the occurrence of the seismic event are associated with the attainment of the limit states for each bridge in the network. In particular, the traffic restriction $d_b=k$ is applied to the b-th bridge if the earthquake induces the damage state $s_b=k$.
The recovery process of each bridge initiates after an idle time and develops over a series of time steps. In the application presented in this paper, the idle time is neglected and the repair actions of each bridge in the network are assumed to start at time t_0. The partial recovery times $t_{p,b}$ are related to time instants in which the attainment of intermediate structural capacity thresholds allows the enforcement of less severe traffic limitations up to complete reopening of the bridge to all users. In particular, $p=1,\ldots,N_{j,b}$ where $N_{j,b}$ is the total number of jumps in the network recovery process. The final recovery time $t_{r,b}$ is associated with the completion of repair actions.
Partial and final recovery times of each bridge depend on both the initial damage and specific repair strategy applied to restore the bridge structural capacity. Furthermore, the initial traffic limitations $d_b=k$ with $k>0$ is partially released through a progressively decreasing sequence of less severe restrictions $d_b=h$ with $k<h$. Finally, full serviceability of the bridge, i.e. $d_b=0$, is assumed to be reached at $t_{r,b}$.

3.2.2 Network Recovery Process and Bridge Recovery Sequences

At the network level, the repair activities on each bridge lead to the definition of a constant stepwise model for the progressive restoration of functionality (Padgett and DesRoches 2007). Therefore, the road network functionality is described by a discrete set of values as a function of the damage state of the bridges, evolving from the initial damage to the fully restored state. The recovery function of network functionality over a time interval $\Delta t_h = t_h - t_0$ between the horizon time t_h and the occurrence time t_0 is hence defined in stepwise form:

$$Q(t) = Q_j \qquad t_j \le t < t_{j+1} \qquad \forall j \in [0, N_j] \tag{13}$$

where $t_j = t_h$ for $j = N_j + 1$ and $N_j = \sum_b N_{j,b}$ is the total number of jumps in the network recovery process. A seismic event occurring at time t_0 causes a sudden drop of network functionality from the pre-event level to $Q_0 = Q(d = s)$ due to the traffic restrictions imposed by the initial damage combination s. Therefore, post-event repair leads to progressive functionality jumps from Q_{j-1} to Q_j at time t_j with $j = 1, \ldots, N_j$.

3.2.3 Resilience Levels and Resilience Measure

The resilience level R_s associated with the initial damage combination s is defined as the integral of the network functionality from the occurrence time to the horizon time t_h normalized by integration time interval. Considering the stepwise form of the network recovery function, the resilience integral can be reduced to the following sum:

$$R_s = \frac{1}{\Delta t_h} \sum_{j=0}^{N_j} Q_j \cdot \Delta t_j \tag{14}$$

where $\Delta t_j = t_j - t_{j-1}$ is the j-th recovery time step and the subscripts d_j with $j = 0, \ldots N_j$ associated with each functionality level Q represent the sequence of network restrictions combination induced by the recovery sequence of each bridge.
Finally, a comprehensive quantification of resilience is obtained weighting the resilience levels R_s with the corresponding probabilities of damage combination in terms of either a pointwise measure associated with the epicenter location $\mathbf{x}_e$ (see Equation 6):

$$R(s|\mathbf{x}_b, t_b, M, \mathbf{x}_e) = \sum_s^{N_s} P_s(s|\mathbf{x}_b, t_b, M, \mathbf{x}_e) \cdot R_s \tag{15}$$

or an average measure over the area source A_s (see Equation 8):

$$R_A(s|\mathbf{x}_b, t_b, M, A_s) = \sum_s^{N_s} P_{s,A}(s|\mathbf{x}_b, t_b, M, A_s) \cdot R_s \tag{16}$$

4. APPLICATION TO A ROAD NETWORK WITH DETERIORATING RC BRIDGES

4.1 RC Box Girder Bridge under Corrosion

The four-span continuous RC bridge shown in Figure 1 is considered (Biondini *et al.* 2015b, Titi *et al.* 2015). The total length of the bridge is 200 m, with spans of 50 m, as shown in Figure 1a. The height of the piers is 14 m. Figure 1b shows the box girder cross-section of the deck. The piers have circular cross-section and are reinforced with 36 steel bars with 30mm-diameter, as shown in Figure 1c (Mander *et al.* 2007). Concrete and steel nominal strengths are f_c=40MPa and f_{sy}=450MPa, respectively.
The piers are assumed to be exposed to a chloride diffusive attack on the external surface, with nominal chloride concentration C_0=3% [wt.%/c]. A nominal diffusivity coefficient $D = 15.8 \times 10^{-12}$ m^2/sec is assumed for concrete. The corrosion damage is evaluated by assuming a nominal damage rate coefficient $q_s = (0.02\ \text{year}^{-1})/C_0$, with corrosion initiation related to the attainment of a nominal critical threshold of concentration C_{cr}=0.6wt.%/c.

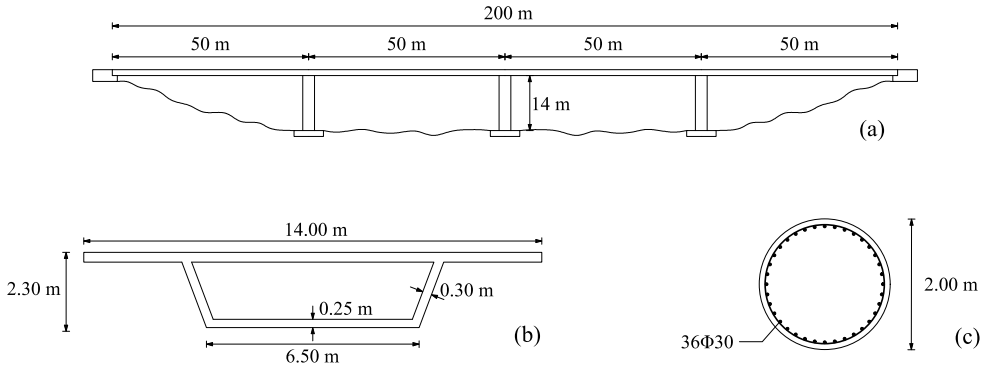

Figure 1. RC box girder bridge: (a) overall geometrical dimensions; (b) deck cross-section; (c) pier cross-section, with reinforcement layout.

4.2 Probabilistic Model

The uncertainties related to the structural system and the damage process are taken into account by assuming uncorrelated probability distributions of the random variables. Nominal values are assumed as mean values. Concrete strength f_c and steel strength f_{sy} are characterized by lognormal distribution with standard deviation of 5MPa and 30MPa, respectively. Chloride critical concentration C_{cr} is described by a beta distribution with coefficient of variation (C.o.V.) of 0.15 and bounds [0.2; 2.0]. Viscous damping ξ, diffusivity D, steel damage rate q_s, and surface chloride concentration C_0 are related to truncated normal distributions (non-negative outcomes) with C.o.V. of 0.40, 0.20, 0.30, and 0.30, respectively. The seismic fragility analysis is carried out by Monte Carlo simulation based on Latin Hypercube Sampling with a sample of 100 realizations of the structural model. Non-linear time-history dynamic analyses are performed for a set of 10 artificial earthquakes generated to comply with the elastic response spectrum given by Eurocode 8 for soil type B (SIMQKE 1976, CEN-EN 1998-1 2004). The values of mean and standard deviation associated with each damage state are listed in Tables 3 and 4 for different bridge ages. Further details can be found in Capacci (2015).

Table 3. Mean value of seismic capacity [g] associated with damage states vs the bridge age.

t_b [years]	0	10	30	60
SD	0.213	0.217	0.228	0.263
MD	0.655	0.626	0.525	0.422
ED	0.819	0.725	0.539	0.424
SC	0.915	0.747	0.540	0.425

Table 4. Standard deviation of bridge seismic capacity [g] associated with damage states vs the bridge age.

t_b [years]	0	10	30	60
SD	0.020	0.019	0.023	0.035
MD	0.060	0.055	0.070	0.075
ED	0.107	0.085	0.086	0.080
SC	0.126	0.103	0.088	0.080

4.3 Bridge Recovery Model

Traffic restrictions are applied to each bridge in the network depending on the initial damage state s_b and on post-event repair actions, which enforce stepwise increments in network functionality when the bridge seismic capacity reaches sufficient levels or residual structural capacity. The assumed partial and final recovery times are listed in Table 5. The horizon time t_h=1 year is also assumed.

Table 5. Partial and final recovery times associated with damage states.

Damage State	$t_{p=1,b}$ [days]	$t_{p=2,b}$ [days]	$t_{p=3,b}$ [days]	$t_{r,b}$ [days]
SD	-	-	-	30
MD	39	-	-	90
ED	82	103	-	180
SC	165	218	262	360

4.4 Road Network and Seismic Sources

The life-cycle resilience of the road network shown in Figure 2 is investigated. The network includes one Origin and one Destination, two identical bridges B1 and B2 built at time $t_{c,1}$=$t_{c,2}$=0 and located on the main highway close to the OD nodes, and a detour route with a re-entry link. Bridges B1 and B2 are located at $\mathbf{x}_{b=1}$=[−5,0] and $\mathbf{x}_{b=2}$=[5,0] (coordinates in km). Table 6 summarizes the traffic parameters of each road segment (main highways, secondary road, re-entry link), including road length L, number of lanes n_L, maximum speed $v_{\max}$, minimum speed $v_{\min}$, critical speed v_{cr}, and minimum distance between vehicles $d_{\min}$. The functionality profile is evaluated based on traffic flow analysis.

Table 6. Network traffic parameters.

Road Segment	L [km]	n_L	$v_{\max}$ [km/h]	$v_{\min}$ [km/h]	v_{cr} [km/h]	$d_{\min}$ [m/cars]
Highway Branch	10	3	130	70	65	30
Secondary Road	40	2	90	50	65	30
Re-entry Link	1	1	90	50	65	30

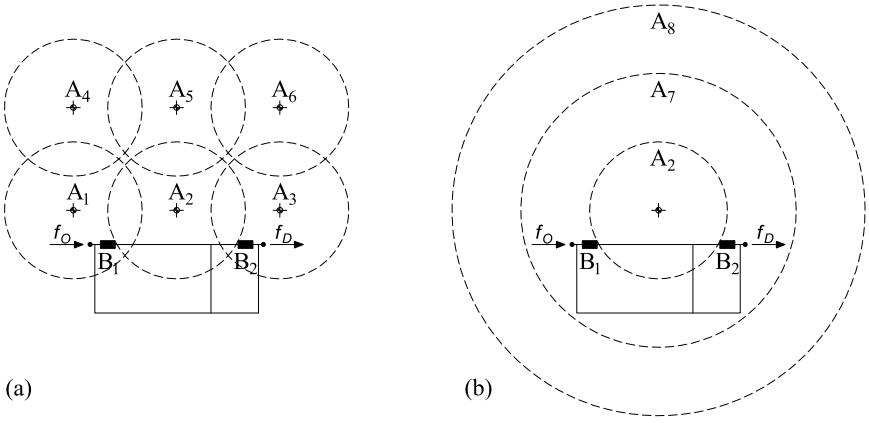

Figure 2. Highway network and area sources.

For a highway network with two bridges (i.e. N_b=2) and five initial damage states (i.e. $N_{s,b}$=5), the number of network functionality profiles is N_s=25. More details on the quantification of the resilience levels associated with each damage combination for the studied network can be found in Biondini *et al.* (2016). Eight circular area sources, with size comparable with the dimensions of the road network, are considered. Figure 2a shows the area sources from A_1 to A_6, characterized by different centers and same radius of 5 km. Figure 2b shows the area sources A_7 and A_8, centered in the same point as the area source A_2 and radius of 10 and 15 km, respectively. Table 7 lists the geometrical parameters of the area sources.

Table 7. Center and size of the area sources.

Parameters	A_1	A_2	A_3	A_4	A_5	A_6	A_7	A_8
x [km]	–9	0	9	–9	0	9	0	0
y [km]	1	1	1	10	10	10	1	1
A_s [km^2]	78.54	78.54	78.54	78.54	78.54	78.54	314.16	706.86

4.5 Seismic Resilience

Figures 3, 4, and 5 show the resilience maps for a seismic event with magnitude M=6.0, 6.5, and 7.0 occurring at time t_0=10, 30 and 60 years, respectively. These maps, obtained considering a square grid of epicenter locations with grid size of 0.2 km, provide a pointwise measure of resilience. It is worth noting that the re-entry link enhances the network redundancy in terms of traffic response, providing a

bypass through undamaged road segments where traffic is impaired by a damaged element. The most important bridge in terms of system functionality and resilience is bridge B_1, which is farther than bridge B_2 from the re-entry link. Such trend is limited for t_0=10 years (Figure 3), since both bridges are not likely to suffer critical corrosion damage. However, it becomes more evident for t_0=30 years (Figure 4) and t_0=60 years (Figure 5), when the structural capacity of both bridges is impaired by corrosion. The thick contour lines shown in Figures 3-5 are related to a resilience level of 90%. It is noted that the region with resilience lower than 90%, embedded by the thick contour lines, is progressively increasing with both earthquake magnitude and lifetime.

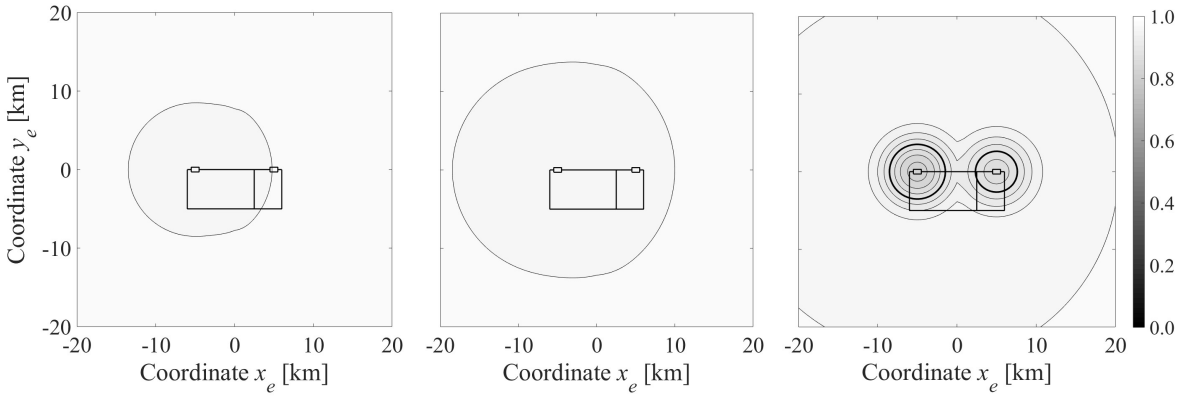

Figure 3. Resilience maps for a seismic event occurring at time t_0=10 years: (a) M=6.0, (b) M=6.5, and (c) M=7.0

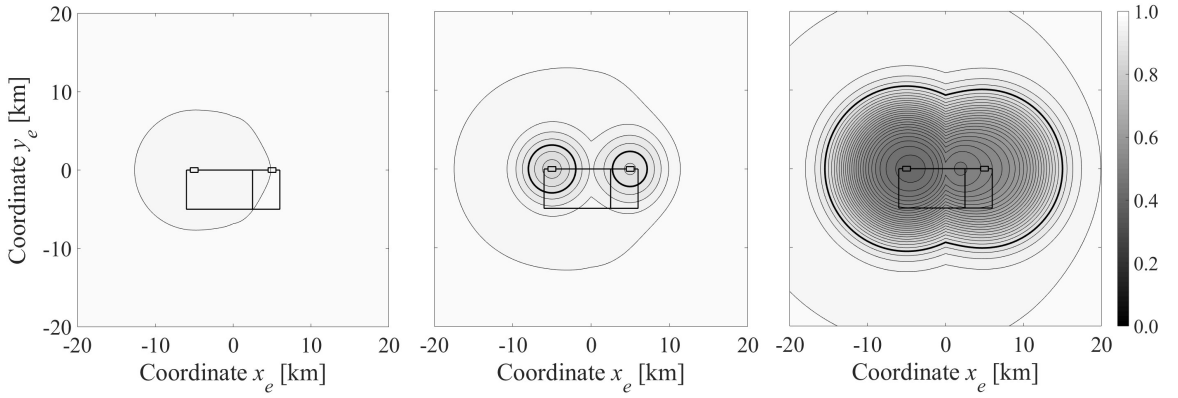

Figure 4. Resilience maps for a seismic event occurring at time t_0=30 years: (a) M=6.0, (b) M=6.5, and (c) M=7.0

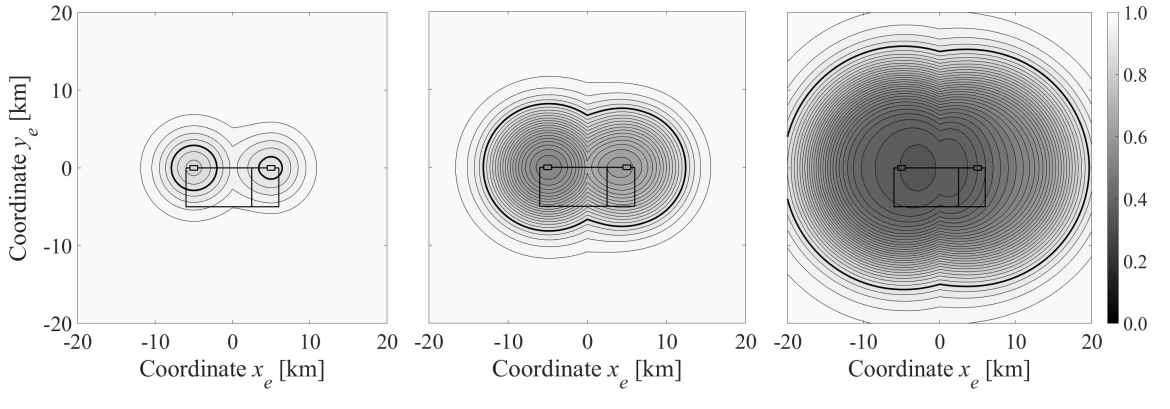

Figure 5. Resilience maps for a seismic event occurring at time t_0=60 years: (a) M=6.0, (b) M=6.5, and (c) M=7.0

The influence of the seismic area source is illustrated in Figures 6 and 7, which show an average measure of seismic resilience versus the occurrence time t_0 for a service life of 100 years. Figure 6 compares the results for the seismic sources A_1, A_2, and A_3 with earthquake magnitude M=6.0, 6.5, and 7.0. The results for area source A_1 show lower resilience values compared to area source A_3 due to the aforementioned topology effect of the re-entry link. Nonetheless, the largest resilience decay rate is associated with area source A_2, since it encloses epicenters that would likely induce severe damage to both bridges. This tendency is emphasized as the earthquake magnitude increases.

Figure 7 compares the results for all the area sources with earthquake magnitude M=7.0. This comparison clearly shows the lower impact of seismic area sources farther from the network centroid, i.e. A_4, A_5, and A_6 compared to A_1, A_2, and A_3. Furthermore, the increase in the size of the area source, i.e. from A_2 to A_7 and A_8, leads to a reduction of the resilience decay rate because larger areas enclose epicenter locations too far from the bridges to induce relevant probability of large damage.

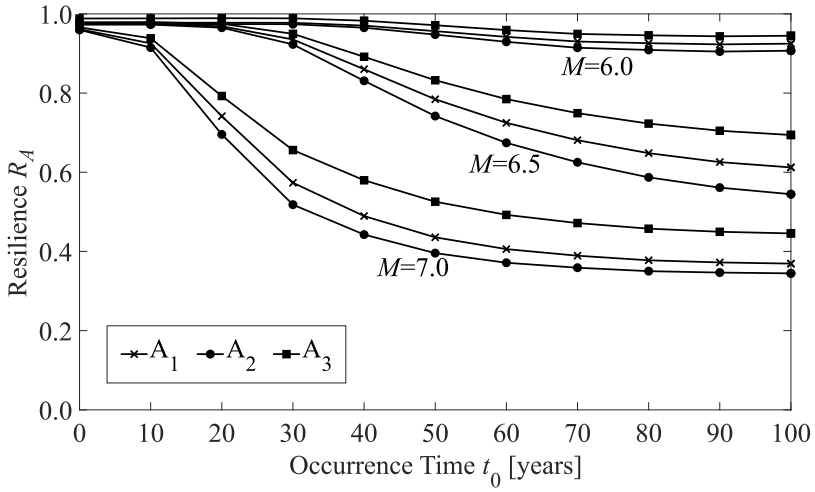

Figure 6. Time-variant resilience for area sources A_1, A_2 and A_3 and earthquake magnitude M=6.0, 6.5, and 7.0

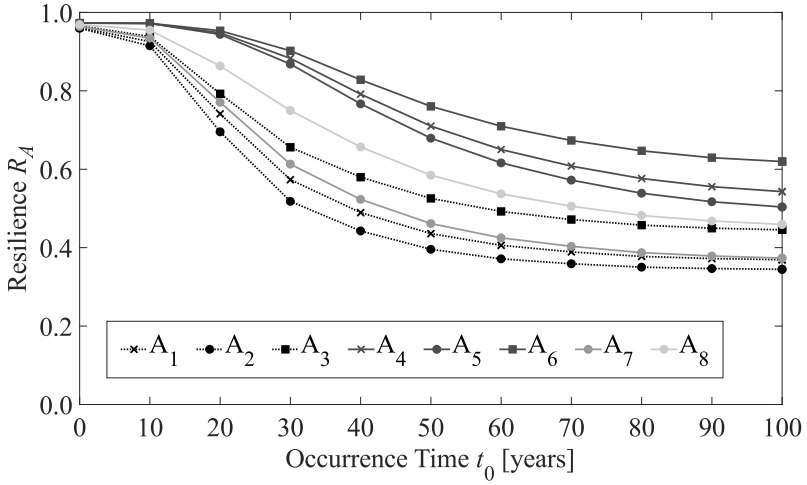

Figure 7. Time-variant resilience for area sources A_1 to A_8 and earthquake magnitude M= 7.0

5. CONCLUSIONS

A probabilistic framework based on seismic capacity assessment of aging bridges and traffic response analysis of transportation infrastructure systems has been developed to measure the life-cycle resilience of highway networks with spatially distributed RC bridges exposed to chloride-induced corrosion and different seismic scenarios. The results of the presented application demonstrated that the proposed

framework can effectively assess the interdependency between seismic hazard scenario, defined in terms of magnitude and epicenter location, and environmental exposure of each vulnerable element in the affected region by means of a congestion-based resilience measure that comprehensively assesses the evolving performance of the transportation lifeline. Severe seismic damage and late restoration can substantially reduce the network resilience due to the application of traffic restrictions that may force traffic flows to be detoured to secondary roads for the time interval required to carry out the necessary repair activities. In general, the decay rate in time of seismic resilience due to aging significantly depends on the seismic exposure in terms of earthquake magnitude, focal distance and geographical features of the seismic source. In particular, the results showed the role of both network topology and location of each exposed bridge under the combined effect of progressive aging and sudden seismic events to identify the most important components in the network.

A comprehensive quantification of resilience has been obtained in terms of either a pointwise measure associated with the epicenter location or an average measure over predefined area sources. Different seismic area sources have been considered to assess the impact of the earthquake scenario, highlighting that both location and size of the area source can affect the resilience measure depending on the reference focal distances of each vulnerable bridge in the network. The proposed approach can assist decision makers in evaluating the effectiveness of proactive mitigation strategies and optimal emergency response in a life-cycle multi-hazard perspective. Specifically, the spatial distribution of vulnerable aging structures and their exposure to hazards can play a key role in assessing proper policies for ex-post interventions, such as prioritizing repair actions, and ex-ante investments, for example aimed at planning retrofit and maintenance of key vulnerable elements or even upgrading the existing network with major infrastructure investments. In this context, downtime and monetary losses associated with the restoration of the structural capacity of critical infrastructure systems should be quantified.

Further research should be devoted to investigate the role of the exposure to disruptive events and the capability of communities to cope with consequences without suffering disproportionate losses with respect to the hazard intensity. Research developments are also needed to characterize the seismic demand at the regional scale, as well as the related impact of cumulative damage induced on vulnerable critical infrastructure components by mainshock-aftershock sequences, site amplification effects and liquefaction, among others, within a life-cycle-oriented multi-hazard approach.

6. REFERENCES

Baker JW (2009). An introduction to probabilistic seismic hazard analysis (PSHA). *White Paper*, version 1.3.

Bertolini L, Elsener B, Pedeferri P, Polder R (2004). *Corrosion of steel in concrete*, Wiley-VCH, Weinheim.

Bindi D, Pacor F, Luzi L, Puglia R, Massa M, Ameri G, Paolucci R (2011). Ground motion prediction equations derived from the Italian strong motion database. *Bulletin of Earthquake Engineering*, 9(6): 1899-1920.

Biondini F, Bontempi F, Frangopol DM, Malerba PG (2004). Cellular automata approach to durability analysis of concrete structures in aggressive environments. *Journal of Structural Engineering*, ASCE, 130(11): 1724-1737.

Biondini F, Camnasio E, Titi A (2015a). Seismic resilience of concrete structures under corrosion. *Earthquake Engineering and Structural Dynamics*, 44(14): 2445-2466.

Biondini F, Capacci L, Titi A (2015b). Seismic resilience of bridges and highway networks. *16th Congress of the Italian Association of Earthquake Engineering*, 13-17 September, L'Aquila, Italy.

Biondini F, Capacci L, Titi A (2016). Seismic resilience of aging bridges and evolving road networks. *5th International Workshop on Design in Civil and Environmental Engineering*, 6-8 October, Rome, Italy

Biondini F, Capacci L, Titi A (2017). Life-cycle resilience of deteriorating bridge networks under earthquake scenarios. *16th World Conference on Earthquake Engineering*, 9-13 January, Santiago of Chile, Chile.

Biondini F, Vergani M (2015). Deteriorating beam finite element for nonlinear analysis of concrete structures under corrosion. *Structure and Infrastructure Engineering*, 11(4): 519-532.

Bocchini P, Frangopol DM (2011). A stochastic computational framework for the joint transportation network fragility analysis and traffic flow distribution under extreme events. *Probabilistic Engineering Mechanics*, 26(2): 182-193.

Bruneau M, Chang SE, Eguchi RT, Lee GC, O'Rourke TD, Reinhorn AM, Shinozuka M, Tierney K, Wallace WA, Winterfeldt DV (2003). A framework to quantitatively assess and enhance the seismic resilience of communities. *Earthquake Spectra*, 19(4): 733-752.

Capacci L (2015). Seismic resilience of bridge networks. *MSc Thesis*, Faculty of Civil Engineering, Politecnico di Milano, Italy.

Capacci L, Biondini F, Titi A (2016). Seismic resilience of aging bridges and transportation networks. *8th International Conference on Bridge Maintenance, Safety and Management*, 26-30 June, Foz do Iguaçu, Brazil.

Capacci L, Biondini F, (2018a). Effects of structural deterioration and infrastructure upgrading on the life-cycle seismic resilience of bridge networks. *IABSE Conference "Engineering the Developing World"*, April 25-27, Kuala Lumpur, Malaysia.

Capacci L, Biondini F, (2018b). Life-cycle seismic resilience of aging bridges and road networks considering bridge capacity correlation. *9th International Conference on Bridge Maintenance, Safety and Management*, 9-13 July, Melbourne, Australia.

Carturan F, Pellegrino C, Rossi R, Gastaldi M, Modena C (2013). An integrated procedure for management of bridge networks in seismic areas. *Bulletin of Earthquake Engineering*, 11(2): 543-559.

CEN-EN 1998-1 (2004). Eurocode 8: Design of structures for earthquake resistance – Part 1: General rules, seismic actions and rules for buildings. European Committee for Standardization, Brussels, Belgium.

Cimellaro GP, Reinhorn AM, Bruneau M (2010). Framework for analytical quantification of disaster resilience. *Engineering Structures*, 32(11): 3639-3649.

Cornell CA (1968). Engineering seismic risk analysis, *Bulletin of the Seismological Society of America*, 58(5): 1583-1606.

Decò A, Bocchini P, Frangopol DM (2013). A probabilistic approach for the prediction of seismic resilience of bridges. *Earthquake Engineering and Structural Dynamics*, 42(10): 1469-1487.

Franchin P, Cavalieri F (2015). Probabilistic assessment of civil infrastructure resilience to earthquakes. *Computer-Aided Civil and Infrastructure Engineering*, Wiley, 30(7): 583-600.

Gilbert SW (2010). Disaster resilience: A guide to the literature. *NIST Special Publication 1117*. National Institute of Standards and Technology, Office of Applied Economics Building and Fire Research Laboratory, Gaithersburg, MD, USA.

Mackie KR, Stojadinović B (2006). Post-earthquake functionality of highway overpass bridges. *Earthquake Engineering and Structural Dynamics*, 35(1): 77-93.

Mander JB, Dhakal, RP, Mashiko N, Solberg KM (2007). Incremental dynamic analysis applied to seismic financial risk assessment of bridges. *Engineering Structures*, 29(10): 2662-2672.

Martin WA, McGuckin NA (1998). Travel estimation techniques for urban planning. *NCHRP Report 365.* Transportation Research Board, Washington DC, USA.

Padgett JE, DesRoches R (2007). Bridge functionality relationships for improved seismic risk assessment of transportation networks. *Earthquake Spectra*, 23(1): 115-130.

SIMQKE (1976). *A program for artificial ground motion generation*. User's manual and documentation. NISEE, Massachusetts Institute of Technology, MA, USA.

Titi A, Biondini F (2013). Resilience of concrete frame structures under corrosion. *11th International Conference on Structural, Safety and Reliability*, 16-20 June, New York, NY, USA.

Titi A, Biondini F, Frangopol DM (2015). Seismic resilience of deteriorating concrete structures, *SEI/ASCE Structures Congress*, 22-25 April, Portland, OR, USA.

Vamvatsikos D, Cornell CA (2002). Incremental dynamic analysis. *Earthquake Engineering & Structural Dynamics*, 31(3): 491-514.

Wardrop JG (1952). Some theoretical aspects of road traffic research. *ICE Proceedings, Engineering Divisions*, 1(3): 325–362.

Zanini MA, Faleschini F, Pellegrino C (2017). Probabilistic seismic risk forecasting of aging bridge networks. *Engineering Structures*, Elsevier, 136(1): 219-232.